Construction and Building Materials 408 (2023) 133687

Contents lists available at ScienceDirect

Construction and Building Materials

journal homepage: www.elsevier.com/locate/conbuildmat

# Thermally induced cracking patterns of the MWCNTs modified cement paste

Maciej Szeląg [a,*], Magdalena Rajczakowska [b], Patryk Rumiński [a], Andrzej Cwirzen [b]

[a] Lublin University of Technology, Faculty of Civil Engineering and Architecture, 40 Nadbystrzycka Str., 20-618 Lublin, Poland
[b] Luleå University of Technology, Department of Civil, Environmental and Natural Resources Engineering, 971 87 Luleå, Sweden

ARTICLE INFO

*Keywords:*
Cement paste
Multiwall carbon nanotubes
Thermal loading
Cracking pattern
Image analysis

ABSTRACT

This paper investigates the influence of the multi-wall carbon nanotubes (MWCNTs) on the structure of cracking patterns (CPs), which is the main novelty, of cement pastes subjected to thermal loading up to 600 °C. The compressive and tensile strength, ultrasonic pulse velocity and weight loss during the thermal loading were investigated. The CPs structure was analyzed using a proprietary digital image segmentation procedure with the use of machine learning algorithms. The total crack area, crack density, fractal dimension and lacunarity of the CPs were determined. In addition, cross sections of cement paste samples were analyzed to determine the average crack depth. The results indicated that the most beneficial MWCNTs content is 0.05 % by weight of cement, for which the increase in the compressive strength was equal 7.8 %. In terms of CPs development, the total crack area and crack density decreased by as much as 41 % at temperatures above 500 °C. At temperatures below 400 °C, MWCNTs increased the crack depth by up to 47.2 %, while at higher temperatures the crack depth decreased to a difference of 1.5 %, compared to the reference cement paste.

## 1. Introduction

Nanotechnology is a growing, multidisciplinary field that deals with the modification, production, design and engineering of materials at the nanoscale level, typically in the range of 1 to 100 nm [1]. At this scale, materials exhibit unique physical, chemical and biological properties that differ from their bulk counterparts [2]. These properties are due to the high surface area-to-volume ratio of nanoparticles [3]. Nanotechnology has found applications in many different fields, including medicine, geotechnics, electronics and materials science [4,5].

One application of CNTs is their addition to cementitious composites (CCs), leading to improved mechanical strength and fracture resistance. Depending on the CNTs type, their content, production method, composition of the concrete mix and the method of testing, the mechanical strength of CCs can increase by as much as 20 % [6]. When using MWCNTs and up to 0.5 % wt. (as in the studies that are the subject of the paper), the increase in the above-mentioned properties may range from 5 to 15 % [7]. Moreover, CNTs can be used as a material for concrete repair, due to their mechanical strength and abrasion resistance. Manzur' et al., [8] investigated Carbon Nanotube Concrete (CNTN) and found that CNTs have good prospects as a material for concrete repair, as such composites showed desirable behavior during setting and in the oblique shear of the material. In addition, due to their unique properties, i.e., conductivity or corrosion resistance, these composites also have applications in corrosion protection of reinforced composites [9,10].

In the manufacturing of CCs with CNTs, they are most often added to the cement mixture in amounts of up to a few percent by weight of cement. Zhang et al., [11] investigated the effectiveness of CNTs in concrete mix by paying attention to the workability of CNTN and different modes of CNTs dispersion. In addition, they analyzed the compressive, tensile, flexural strength and dynamic impact resistance of CNTs. The results showed that the addition of CNTs mostly reduces the workability of concrete, but dispersed agglomerates of CNTs relatively increase fluidity. The mechanical properties show a tendency to initially increase and then decrease, so the optimal content of CNTs in the samples was 0.10 %-0.20 % by weight of the cement. In addition, it has been observed that CNTs can fill internal pores, leading to a reduction in porosity and limiting the penetration of chloride and sulfate ions into the material.

Dispersion of CNTs in CCs is crucial to obtain a homogeneous composite structure that will provide the desired mechanical and physical properties [12,13]. One of the most common ways to disperse CNTs in a

* Corresponding author.
*E-mail addresses:* maciej.szelag@pollub.pl (M. Szeląg), magdalena.rajczakowska@ltu.se (M. Rajczakowska), p.ruminski@pollub.pl (P. Rumiński), andrzej.cwirzen@ltu.se (A. Cwirzen).

https://doi.org/10.1016/j.conbuildmat.2023.133687
Received 23 May 2023; Received in revised form 2 October 2023; Accepted 4 October 2023
Available online 10 October 2023

CCs is the dispersion method. It involves preparing an aqueous dispersion of CNTs with surfactant and then combining it with cement and the other components of the composite. To prepare the CNTs dispersion, the sonication process is frequently carried out [14–17].

CNTs can improve its resistance to high temperatures. CNTs have very good thermal properties, so they can act as an excellent reinforcing material to prevent deformation and cracking of the composite due to high/low temperatures. CNTs can lead to a reduction in the thermal expansion of the composite, which minimizes the risk of its cracking and damage [12]. According to Baloch [18], the main mechanism for limiting CCs cracks is the bridging action, which can result in an average decrease in crack width up to 15 %. This significantly increases the tightness and durability of CCs.

The introduction of CNTs into CCs can also affect their thermal properties by increasing their thermal conductivity [19,20]. CNTs have very good thermal conductivity which results in the formation of a thermally conductive network in CCs. The increase in thermal conductivity has important applications for composites significantly exposed to high temperatures, such as fireproof materials or structural components in high-rise buildings or other places where temperatures can reach very high values [21,22].

The most common defects in the structure of a cement paste are cracks. In the case of cement pastes and other CCs, the appearance of cracks in the material is particularly dangerous since these materials are inherently brittle. This usually results in the sudden and explosive failure of the material when the development of cracks leads to exceeding its load-bearing capacity. One way to evaluate the durability of a cracked material is to analyze its cracking pattern (CP), resulting from external loading. This research area has been developing strongly in recent years [23,24]. Since the subject of analysis in this paper are CPs induced by thermal loading, considerations have been limited to this area. Studies by other researchers prove that CPs analysis allows evaluating the degree of degradation of a cementitious material globally and in relation to its physico-mechanical properties [25,26]. The CPs structure affects virtually every aspect of the CCs durability, from mechanical strength through, e.g., waterproofing or resistance to chemical corrosion.

There are very few research that analyze the CPs structure of CCs with the addition of multi-wall carbon nanotubes (MWCNTs). In the work [27], a cement paste modified with MWCNTs with three different w/c ratios = 0.4, 0.5, and 0.6, thermally loaded, was studied. The MWCNTs were introduced into the structure of the cement matrix as an aqueous dispersion in the presence of the surfactant – sodium dodecyl sulfate (SDS). The application of SDS caused foaming of the cement matrix and a radical change in the physico- mechanical properties of the cement paste, which had a great impact on CPs. The application of MWCNTs in the presence of SDS resulted in a significant reduction in the crack density (CD), i.e., up to 50 %. A study by Kim et al., [28] shows that in cementitious pastes thermally loaded above 900 °C, massive CP is formed in the edge zone of the material. This has been identified as the main cause of explosive spalling.

The main aim of the study was to analyze the CPs development of cement pastes with MWCNTs, as a function of thermal loading, and then attempt to relate the CPs structure to the mechanical properties of the cement pastes. Above is the main novelty of the paper. There is a lack of information in the literature regarding the impact of MWCNTs on the CPs structure, and this has a key factor which determines the durability of CCs under thermal load conditions. Therefore, conducting research in this field was considered reasonable and cognitive from a scientific point of view. MWCNTs were incorporated into the structure of the cement matrix as an aqueous dispersion in the presence of a polycarboxylate-based surfactant. Five series of cement pastes differing in the content of MWCNTs, in the amount of 0–0.3 % relative to the weight of cement, were studied at temperatures from 50 °C to 600 °C. In addition to the CPs quantitative characterization, the basic mechanical properties, which are a measure of the thermal degradation of the cement paste, were examined. The results indicated that in terms of mechanical strength, the most optimal MWCNTs content was 0.05 wt%. CP analysis indicated a beneficial effect of MWCNTs only from 400 °C onward by reducing the complexity of the cracks structure and reducing the average cracks depth.

The study is a continuation of the research presented in [29]. The same recipes of MWCNTs cement paste and the same thermal load regime were applied, but the aim of the research was different. In contrast, in research [29] the aim was to evaluate the process of autogenous self-healing of thermal cracks (in the range of 200–400 °C), by means of the crack closure measurements.

## 2. Materials and methods

### 2.1. Materials

The Ordinary Portland Cement (OPC) CEM I 42.5 N from Cementa Heidelbergcement Group, (Stockholm, Sweden) was used in the study. The OPC used is characterized by the following chemical composition (given in the oxide equivalents): CaO = 63.3 %, $SiO_2$ = 21.2 %, $Al_2O_3$ = 3.4 %, $Fe_2O_3$ = 4.1 %, MgO = 2.2 %, $Na_2O$ = 0.18 %, $K_2O$ = 0.56 %, $SO_3$ = 2.7 %, and Cl < 0.01 %. The loss on ignition (LOI) is 2.5 %.

The NC7000 multi-wall carbon nanotubes (MWCNTs) manufactured by the Nanocycl SA (Sambreville, Belgium) were used as a nano-reinforcement of the cement paste. The MWCNTs used are not surface functionalized. Their average diameter is 9.5 nm, average length – 1.5 μm, carbon purity – 90 %, metal oxide – 10 %, specific surface area – 250–300 $m^2$/g.

### 2.2. Specimens preparation

The process of preparing samples was divided into two stages, i.e., the first – preparation of an aqueous dispersion of MWCNTs, and the second – preparation of cement paste. It is well known that MWCNTs, due to their very large specific surface area (>250 $m^2$/g), have a strong tendency to agglomerate into larger clusters [30]. Directly adding them to cement and mixing them mechanically would have no effect, since the beneficial effect of their use is visible only when they are highly dispersed in the volume of the cement matrix. Studies available in the literature [31] indicate that one possibility to obtain a stable dispersion of MWCNTs is their sonication in water in the presence of a polymer, such as: a polycarboxylate-based admixture. Thus, the commercially available polycarboxylate-based superplasticizer Sika ACE 30 (Baar, Switzerland) was used as the surfactant. Importantly, literature studies [32] indicates a high stability of the MWCNTs-polycarboxylate-based superplasticizer dispersion. A number of tests were performed and a final MWCNTs:surfactant mass ratio of 1:2 was determined. Initially, the target amount of surfactant was premixed in water, then MWCNTs were added and the resulting solution was sonicated using a Hielscher Ultrasonics sonicator UP200St (Teltow, Germany). Each time to obtain the same degree of dispersion of MWCNTs, an equal amount of dispersion was sonicated, i.e., enough to produce 3 samples for testing – each time it was 510 g of water and, depending on the formulation, an appropriate amount of polymer and MWCNTs. The final sonication time was 10 min with a sonotrode vibration amplitude of 100 %. The stability of the MWCNTs dispersion thus obtained was monitored for 26 days visually. During this time, no segregation of the dispersion components was observed. The dispersion thus formed was then combined with cement and mechanically mixed for a period of 3 min in a Hobart mixer. The paste was then placed in two layers successively compacted on a vibrating table, in 40x40x160 mm molds. The samples were unmolded after 24 h, and then matured for a period of 28 days in a water bath at about 20 °C.

A total of 5 series of cement pastes differing in the percentage of MWCNTs relative to the weight of the cement, i.e., MWCNTs at 0.05 % wt., 0.1 %wt., 0.2 %wt. and 0.3 %wt. respectively, were made and tested. The mix details are provided in Table 1. In addition, a reference series, i.e., pure cement paste, without MWCNTs, was also made. The series were designated C-0 (reference), C-0.05, C-0.1, C-0.2, and C-0.3, respectively. The cement paste was made with a constant water/cement ratio (w/c) of 0.4. The MWCNTs ratio was selected on the basis of studies available in the literature, which indicate that the greatest benefits, in terms of improved physical and mechanical properties, of applying MWCNTs to cement pastes are obtained when they are applied up to 0.5 %wt.[11]. See (Table 2).

### 2.3. Thermal loading

Cement pastes with MWCNTs were loaded with elevated temperatures in several variations, i.e., 50 °C (dried to a constant weight), 200 °C, 300 °C, 400 °C, 500 °C, and 600 °C. The thermal loading procedure consisted of preheating the oven to the target temperature, then a set of samples was placed in the oven and heated for a period of 2 h. After this time, the samples were removed from the furnace and cooled by a natural temperature drop. All samples were dried to a constant weight at 50 °C before thermal loading. This was to protect against intense vapor pressure buildup inside the sample, which could result in the sample exploding in the furnace and ultimately destroying it. The insertion of the specimens into the preheated furnace corresponds to loading conditions based on a thermal shock, which the authors of this paper have already used in previous studies on cracking patterns of modified cement pastes [33,34]. The study conducted is more of a cognitive nature, so the adopted scope and method of thermal loading does not correspond to the application fire resistance studies.

### 2.4. Test methods

#### 2.4.1. Mechanical and physical properties

The tensile strength ($f_{cf}$) was tested in a three-point bending scheme according to the EN 12390–5 [35]. Then, the compressive strength ($f_c$) was tested on the halves of the specimens formed after the $f_{cf}$ test, according to the EN 12390–3 [36]. Strength tests were carried out using a universal loading machine (Wykeham Farrance) combined with a 50 kN loading cell and the QuantumX MX440B universal measuring amplifier (HBM, Darmstadt, Germany). In addition, before and after the thermal loading process, the weight of the samples was tested to obtain information regarding the weight loss due to the thermal loading (ΔM). The ultrasonic pulse velocity (UPV) was also investigated using a Proceq Pundit Lab with 54 kHz transducer. The results obtained are the average of 3 samples and for $f_c$ – 6 samples.

#### 2.4.2. Cracking patterns measurements

To analyze the CPs, the bottom surface of the specimen relative to the molding direction was scanned on an optical scanner at a resolution of 1200 DPI (47.2441 px/mm). This made it possible to obtain a highly detailed image of the cracked surface of the cement paste. The binary image of the CPs was obtained by implementing an image segmentation procedure using machine learning algorithms, in the Trainable Weka Segmentation Fiji software plugin with ImageJ [37]. The digital image segmentation procedure applied is described in detail in [38,39]. The following parameters were used to quantitatively describe the CPs structure:

- TCA – total cracks area [$cm^2/m^2$], which was calculated as the ratio of the area occupied by cracks to the total area of the image,
- CD – cracks density [1/m], calculated as the number of cracks crossing a test line of known length,
- $FD_B$ – fractal dimension of the cracking patterns [-], calculated using the box-counting method with the FracLac for ImageJ [40],
- LAC – lacunarity of the cracking patterns [-], calculated as an alternative fractal dimension also using the box-counting method with the FracLac for ImageJ [40].

To supplement the results obtained the analysis of the density distribution of the above quantities has been also performed. In addition, cross sections of thermally loaded cement paste samples with MWCNTs were analyzed. The analysis was aimed at determining the depth of cracks as a function of thermal loading. After scanning the surfaces of the specimens for cracking patterns analysis, a portion of the test specimen was dipped in epoxy resin to protect the crack structure from further development. After the resin hardened, the cross-section was cut using a diamond circular saw and was polished using Struers CitoVac and Labosystem (Struers, Ballerup, Denmark). The resulting cross-sections were then scanned on an optical scanner at 1200 DPI resolution and further analyzed using a Dino-Lite Pro AM-413 T portable digital optical microscope. This allowed the average crack depth (ACD) to be determined as a function of thermal loading.

**Table 1**
Mix details of the MWCNTs modified cement pastes.

| Series designation | Amount of ingredients [g] for single batch (3 samples 40x40x160 mm) | | | |
|---|---|---|---|---|
| | Cement | Water | Surfactant | MWCNTs |
| C-0 | 1275 | 510 | – | – |
| C-0.05 | 1275 | 510 | 1.275 | 0.638 |
| C-0.1 | 1275 | 510 | 2.550 | 1.275 |
| C-0.2 | 1275 | 510 | 5.100 | 2.550 |
| C-0.3 | 1275 | 510 | 7.650 | 3.825 |

## 3. Results and discussion

### 3.1. Effect of loading temperature on basic properties

#### 3.1.1. Compressive strength

Fig. 1 shows the results of compressive strength of cement pastes modified with MWCNTs, as a function of thermal loading.

The highest $f_c$ value was found for 0.05 wt% MWCNTs content (C-0.05) under 300 °C thermal loading, which is 66.8 MPa. On the other hand, the lowest $f_c$ was found for 0.3 wt% MWCNTs content (C-0.3) at a thermal load of 600 °C, which is 28.0 MPa. The MWCNTs addition relatively increased the $f_c$ of the cement pastes. The MWCNTs content of 0.05 % was the most favorable in this case. The C-0.05, C-0.1, and C-0.2 series obtained $f_c$ values on average 7.8 %, 2.0 %, and 1.4 % higher compared to C-0. In contrast, the cement paste with the highest amount of carbon nanotubes (C-0.3) had a worse compressive strength, averaging 2.3 % higher compared to C-0. In this case, too high content of MWCNTs in the cement matrix can result in problems in their dispersion. Thus, agglomerates of MWCNTs are formed, which cause a break in the continuity of the structure and a decrease in the cohesion of the cement matrix. This fact was also confirmed by the cross-sectional analyses described further in Section 3.3 of the paper. For example, Chaipanich et al., [41] showed that the addition of MWCNTs increased the $f_c$ of cement mortars. The highest strength was obtained for mortars with 20 % fly ash by weight and 1 % of MWCNTs, where the $f_c$ after 28 days was 51.8 MPa. It was found that a good interaction between MWCNTs and the cement matrix with fly ash is evident when MWCNTs act as a filler creating nucleation sites for hydration products. This resulted in a denser microstructure and higher strength compared to a reference mix without MWCNTs.

Thermal loading had the greatest effect on $f_c$. Increasing the temperature to the 300 °C resulted in higher $f_c$ values. After 200 °C and 300 °C, $f_c$ values were 8.2 % and 6.5 % higher, respectively, compared to samples dried at 50 °C only. This is related to the effect of internal autoclaving of the cement matrix structure, which is also confirmed by other studies [42]. In this temperature range, the thermal degradation of the cement matrix is small, while the resulting steam pressure causes further intensive hydration of the hitherto non-hydrated parts of the

**Table 2**
Percentage change in the quantitative properties of CPs, depending on MWCNTs content and loading temperature, with respect to the reference series – CP-0.

| Temp. [°C] | Series | TCA [%] | CD [%] | $FD_B$ [%] | LAC [%] |
|---|---|---|---|---|---|
| 50 | C-0.05 | 35.5 | 14.1 | 2.2 | 3.8 |
| | C-0.1 | 15.0 | 5.6 | 2.7 | -9.8 |
| | C-0.2 | 38.1 | 51.2 | -0.5 | -1.7 |
| | C-0.3 | 59.8 | 45.6 | 3.5 | -7.9 |
| 200 | C-0.05 | 29.8 | 13.2 | 2.0 | 2.0 |
| | C-0.1 | 17.1 | 13.2 | 1.2 | 0.6 |
| | C-0.2 | 32.1 | 31.1 | -1.6 | 3.9 |
| | C-0.3 | 56.5 | 24.4 | 3.1 | -9.1 |
| 300 | C-0.05 | 10.4 | -3.5 | 2.1 | -22.2 |
| | C-0.1 | -6.8 | -0.1 | -1.9 | 0.3 |
| | C-0.2 | 10.4 | 10.3 | -0.4 | -9.5 |
| | C-0.3 | 27.5 | 20.7 | 0.0 | -4.8 |
| 400 | C-0.05 | 1.2 | -9.5 | 1.8 | 0.8 |
| | C-0.1 | 7.4 | 11.9 | -1.1 | 10.2 |
| | C-0.2 | -6.0 | -3.5 | -0.1 | -0.8 |
| | C-0.3 | 6.9 | -1.2 | 1.0 | -4.4 |
| 500 | C-0.05 | -2.3 | -16.2 | 5.1 | -14.5 |
| | C-0.1 | -6.8 | 4.4 | 1.5 | -4.7 |
| | C-0.2 | -5.0 | -17.6 | 2.4 | 0.6 |
| | C-0.3 | 8.1 | -10.3 | 5.9 | -19.1 |
| 600 | C-0.05 | -16.1 | -6.7 | -4.7 | 4.7 |
| | C-0.1 | -10.6 | -6.7 | -4.3 | 13.4 |
| | C-0.2 | -17.1 | -20.3 | -2.4 | -14.7 |
| | C-0.3 | -41.5 | -40.7 | -8.4 | 1.6 |

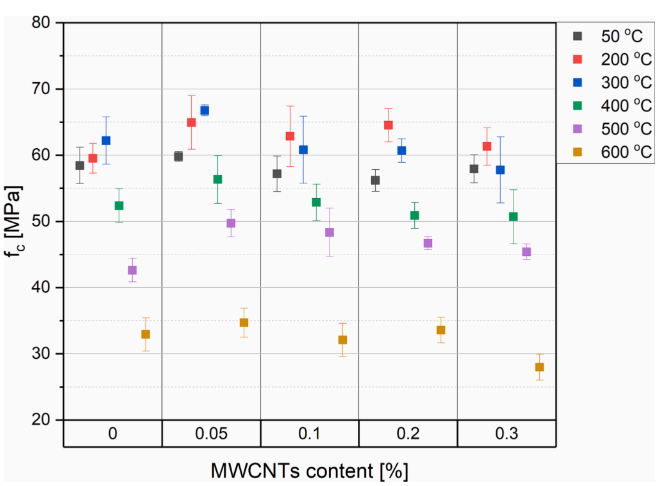


**Fig. 1.** Compressive strength of cement paste with MWCNTs after 28 days.

cement grains, which ultimately increases $f_c$. On the other hand, after loading at 400 °C, 500 °C, and 600 °C, progressive thermal degradation of cement pastes with MWCNTs can be seen. The $f_c$ values were successively lower, on average by 9.1 %, 19.6 %, and 44.2 %, compared to 50 °C. The $f_c$ values after 200 °C and 300 °C are mostly similar to each other in terms of MWCNTs content. Only above 500 °C there was a uniform decrease in $f_c$ as the percentage of MWCNTs increased. The values of the coefficient of variation for $f_c$ were below 8.3 %, indicating the high reproducibility of the results. On the other hand, a study by Irshidat et al., [43] shows that MWCNTs exhibit the ability to increase the $f_c$ of cement matrix exposed to elevated temperatures up to 600 °C. However, this improvement was less significant at temperatures higher than the melting point of the fibers. It was verified that a plain unheated sample of ordinary cement mortar had a compressive strength of 30 MPa. When 0.05 % CNT was introduced in combination with 0.1 % polypropylene (PP) fibers by weight of cement, the $f_c$ increased by almost 30 %. By increasing the thermal loading to 200 °C, the samples showed another increase in $f_c$, which was related to the continuation of the hydration process of the cement particles by heating. At higher temperature loads, a decreasing trend in $f_c$ was found for the reference samples and those with MWCNTs and PP. However, the samples with MWCNTs and PP retained only 49 % of their original $f_c$ after reaching 600 °C. Compared to the reference samples, these retained only 33 % of the initial $f_c$ value.

### *3.1.2. Tensile strength*

Fig. 2 shows the tensile strength ($f_{cf}$) of cement pastes modified with MWCNTs. Tensile strength, in the case of thermally loaded cement pastes, is strongly dependent on the location of structure defects in the volume of the material. The most important is the location of thermal cracks, which means that, by nature, $f_{cf}$ results after thermal loading can have significant discrepancies. An increase in the MWCNTs content in the cement matrix significantly affects the $f_{cf}$ of cement pastes. The largest percentage increase (41 %) in $f_{cf}$ was recorded for C-0.3 (1.22

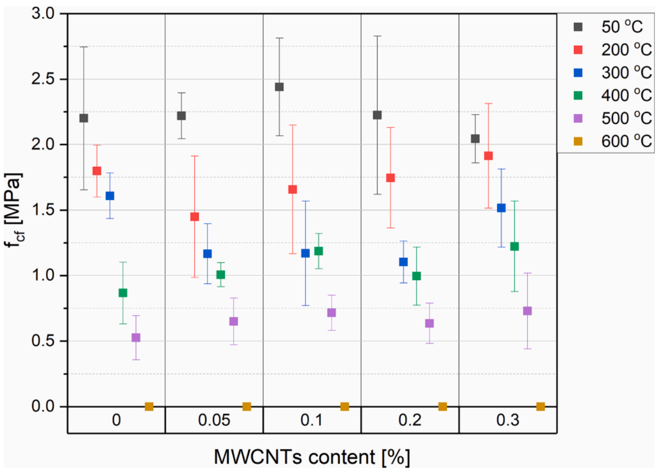


**Fig. 2.** Tensile strength of cement paste with MWCNTs after 28 days.

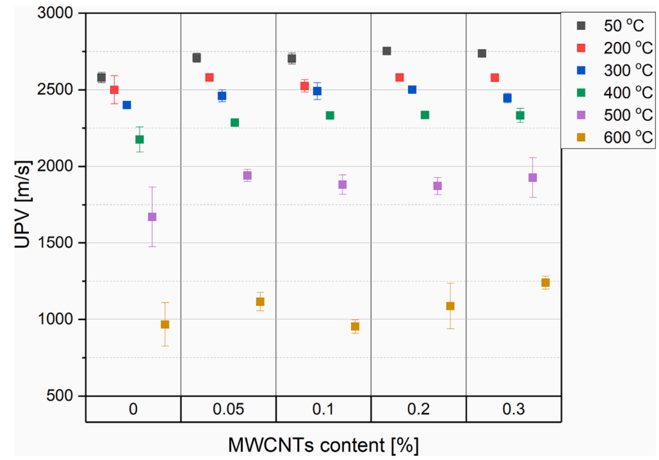


**Fig. 3.** Ultrasonic pulse velocity (UPV) of cement pastes with MWCNTs.

MPa) relative to the reference series (0.87 MPa), under thermal loading of 400 °C. The C-0.1 series at 50 °C load showed the highest $f_{cf}$ in the study equal to 2.44 MPa. Yet this is the only case for which the $f_{cf}$ value for 0.1 % MWCNTs was higher than the other series with MWCNTs. It should be noted that all mixtures under 600 °C reached a value below the machine detection limit. The cement pastes, while characterized by residual compressive strength, broke in the hands. The reason for this is, firstly, the thermal cracks structure, and secondly, the significant chemical degradation of the cement matrix. For this reason, the highest $f_{cf}$ values were obtained at a thermal load of 50 °C. The percentage difference for C-0 against the maximum $f_{cf}$ value (2.20 MPa for 50 °C) and the minimum registered value (0.53 MPa for 500 °C) is as high as 317.8 %. For the C-0.3 series, the difference is 180.1 %. The higher MWCNTs content influences the relative increase in $f_{cf}$, especially at higher thermal loads. For example, cement pastes with MWCNTs showed higher $f_{cf}$ values by an average of 27.2 % and 29.7 % compared to C-0 after thermal loading at 400 °C and 500 °C. Thermal degradation reveals the positive effect of MWCNTs, which most likely bridge the microcracks in the degraded structure of the cement matrix. For comparison, Cui et al., [44] showed that the $f_{cf}$ for cementitious composites reaches a maximum at 0.5 % MWCNTs content, which meant a 21.8 % increase in $f_{cf}$ relative to the reference samples.

In the extreme case, the coefficient of variation reached 31 %, and for each series it became larger and larger as the loading temperature increased. This confirms how strongly the location and orientation of cracks in the cement paste affects the repeatability of $f_{cf}$ results as a function of thermal loading.

### 3.1.3. Ultrasonic pulse velocity

With an increase of the thermal loading, a decrease in the ultrasonic pulse velocity (UPV) was observed (Fig. 3). Due to the relatively linear increases in UPV relative to the MWCNTs content, temperature is the main factor affecting the change in UPV. It was also found that increasing the MWCNTs content increased the UPV value. The C-0.05, C-0.1, C-0.2, and C-0.3 series obtained UPV values that were on average higher by 6.5 %, 4.8 %, 6.8 %, and 7.9 %, respectively, compared to C-0. Increasing the content of MWCNTs reduced the porosity of the cement composite, which directly results in increased UPV values. This reduced porosity may also be due to the fact that MWCNTs act as nucleation sites for cement hydration products, which directly translates into the sealing of the microstructure and its local increase in density. This is also confirmed by Leonavičius et al., [45], who showed an increase in UPV for samples containing lower amounts of CNTs compared to reference samples. The UPV after 28 days of maturation for samples with 0.005 wt % MWCNTs was 4170–4240 m/s, which was greater by 4.2 % compared to the reference samples. In samples with higher CNTs content, the UPV increased to 4040 m/s and 4020 m/s, i.e., 0.73 % and 1.23 % less compared to the reference samples. Most significant in the context of UPV is the change associated with the impact of increased temperature. The less dense the medium (more pores, voids, cracks), the slower the propagation speed of the ultrasonic wave through the material. UPV values were on average 5.3 %, 8.8 %, 15.0 %, 31.1 %, and 60.2 % lower for measurements taken at 200 °C, 300 °C, 400 °C, 500 °C, and 600 °C, respectively, compared to 50 °C.

The UPV test was characterized by a very high reproducibility of the results, as the coefficient of variation was obtained in most cases less than 4 %. Only for measurements after 600 °C this value was slightly exceeded, which is related to the strongly developed structure of thermal defects. The relationships of UPV-$f_c$ and UPV-$f_{cf}$ were characterized by a very strong correlation. The values of Pearson's correlation coefficients were 0.94 and 0.92, respectively. The high correlation between UPV and the mechanical properties of cement composites is also confirmed by other studies [46,47].

### 3.1.4. Weight loss due to the thermal loading

The decrease in weight (ΔM) of cement pastes as a function of thermal loading is mainly related to the evaporation of free and physically bounded water with increasing temperature (Fig. 4). No effect of MWCNTs content on ΔM was observed. The ΔM was very similar for all series within a single thermal load, i.e., after 200 °C – 4.3–5.0 %, after 300 °C – 9.1–9.6 %, after 400 °C – 11.8–12.8 %, after 500 °C – 13.3–14.1

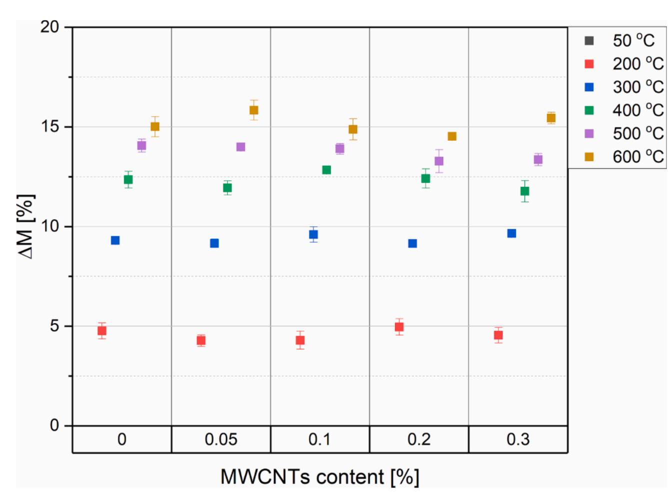


**Fig. 4.** Weight loss (ΔM) of cement pastes with MWCNTs as a function of thermal loading.

%, and after 600 °C – 14.5–15.8 %. The reference point is the weight of the samples after drying at 50 °C. The greatest dynamics of weight decrease occurs during the initial periods of heating, then the largest amounts of water are removed from the material in the form of water vapor.

### 3.2. Evolution of the cracking patterns

Fig. 5 shows the quantitative properties of cracking patterns (CPs) of cement pastes modified with MWCNTs as a function of thermal load. What is observable is the development of the CPs structure as a function of thermal load up to 400–500 °C, after which, at 600 °C, the results indicate a change in a nature of the thermal CPs of the cement matrix. The results obtained at 50 °C are considered as reference results, since this is the state of the material after the drying process, even before the main thermal load. The cracks formed at this stage are mainly the result of thermal shrinkage associated with the slow evaporation of free water [48]. Analyzing the results without considering the MWCNTs content, it was found that the TCA increases stably up to 400 °C. The increase is 50.8 %, 113.4 %, and 189.2 %, for temperatures of 200 °C, 300 °C, and 400 °C, respectively. Thus, for 400 °C, an almost 3-fold increase in the area occupied by cracks was observed compared to the initial state. Analogous is the case of CD, the increase in CD at 200 °C, 300 °C, and 400 °C is 21.3 %, 41.7 %, and 93.5 %, respectively. The much larger relative increase in TCA compared to CD as a function of thermal load indicates that the process of propagation and evolution of already existing cracks dominates, rather than the process of formation of new thermal cracks. This is due to the fact that less energy needs to be supplied to the system for the evolution of an already existing cracks than for the generation of new cracks. This is also confirmed by other researchers [49]. On the other hand, the difference in TCA for temperatures of 400 °C and 500 °C was practically negligible, while a decrease in CD values was observed. Virtually the same crack area with a simultaneous decrease in their degree of density indicates the formation of fewer cracks of significant width. This is a phenomenon that directly influences the increasing reduction of $f_c$ and $f_{cf}$ at 500 °C, as reflected in the results of the mechanical properties of cement pastes with MWCNTs described earlier. At 600 °C, on the other hand, both a decrease in TCA and CD values were observed relative to 400 °C and 500 °C. It should be mentioned, however, that the formation of very fine structure cracking patterns was observed during the study, the quantitative characterization of which could not be captured by the test method used due to the very small crack widths. When scanning at a resolution of 1200 DPI and assuming positive identification of a crack with a minimum width of 2 px, this results in the identification of cracks with a width of min. 42 μm. However, the strong development of the CPs as well as the intensifying process of chemical degradation of the cement paste. This can be considered the same as the breakdown of the main cementitious phases, starting at 460 °C in the case of portlandite. The ultimate effect is a radical decrease in the cohesion of the material that leads to its complete destruction. Studies by Naus et al., [50] indicate that the main reason for the mechanical degradation of cement paste is a significant increase in thermal deformation.

Earlier studies conducted by the authors [39] as well as research conducted by Farhidzadeh et al., [51] prove that the CP that forms on the surface of cementitious composites subjected to external loading is fractal in nature. Its degree of complexity can be described by, e.g., the fractal dimension. In the study, it was observed that the development of

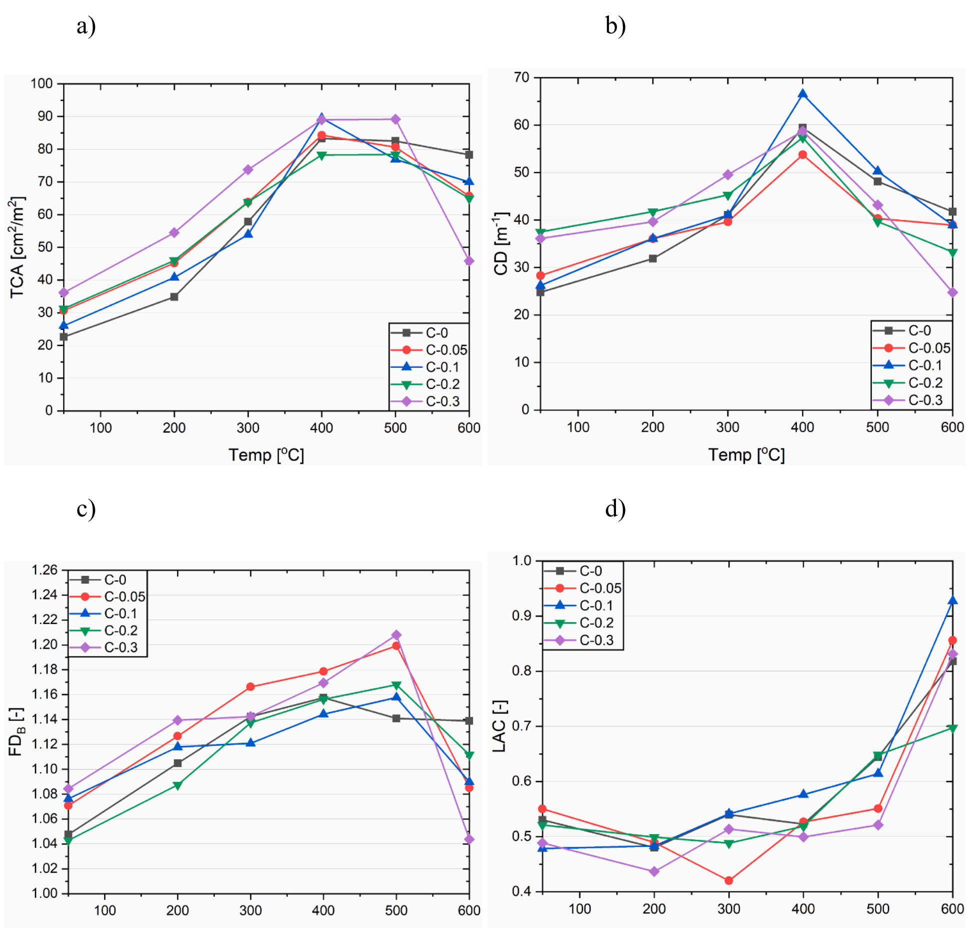


**Fig. 5.** Properties of the cracking patterns: a) TCA; b) CD; c) $FD_B$; d) LAC.

the CPs complexity occurred uniformly and stably up to 500 °C, after which at 600 °C the value of $FD_B$ decreased, similar to the TCA and CD. The average increase in $FD_B$ value at 200 °C, 300 °C, 400 °C, and 500 °C, relative to 50 °C, was 4.8 %, 7.3 %, 9.1 %, and 10.4 %, respectively (Fig. 5c). As mentioned above, up to 400–500 °C, the cement matrix is thermally stable, i.e., chemical cohesion is largely preserved, and the degradation of the material and the CP development occurs mainly due to the evaporation of initially free water, surface water, and then capillary-bound water. The resulting vapor pressure gradient in the cement matrix volume results in the occurrence of increasing thermal deformation [52]. The decrease in the $FD_B$ at 600 °C confirms the fact that there are fewer cracks on the surface of the cement matrix, but with significant widths.

The lacunarity (LAC) (Fig. 5d) of the CPs structure was also evaluated in the conducted study. To date, it has not been reported in the literature that LAC has been used to characterize the structure of thermal cracks formed in cement pastes. LAC is one of the measures of the fractal dimension and refers to the presence of voids or gaps between elements of a fractal. If a fractal contains a large number of gaps, it means that its fractal dimension is smaller than if the gaps are not present. In other words, lacunarity reduces the complexity of a fractal and affects its mathematical properties. Moreover, the more homogeneous the analyzed structure is, the smaller the LAC values are [53]. The nature of the changes in LAC values depended on the value of thermal loading. Treating the values obtained for 50 °C as the reference condition, a decrease in LAC values was found first by an average of 7.0 % (200 °C) and then by 2.5 % (300 °C). Starting at 400 °C, the LAC values of the CPs increased on average by 2.9 %, and further by 16.0 % (500 °C) and finally by as much as 60.8 % (600 °C). The results obtained in this range are strongly correlated with $f_c$ and UPV, the basic mechanical properties of cement paste. The Pearson's correlation coefficients are −0.90 (LAC-$f_c$) and −0.91 (LAC-UPV), respectively. In the course of the study, it was noted that of all the parameters quantitatively characterizing the CPs, LAC is the parameter most strongly correlated with the mechanical parameters of cement pastes modified with MWCNTs. As stated earlier, up to 300 °C, there was an autoclaving phenomenon of the cement matrix, which positively affected $f_c$. The obtained LAC results, indicate that the increase in $f_c$ is strongly related to the increase in the degree of structural homogeneity of the CPs.

Fig. 6 shows the density distribution of the coefficient of variation (V) for the individual measures used to describe the CPs. The analysis of the density distribution of V is of great practical importance because it

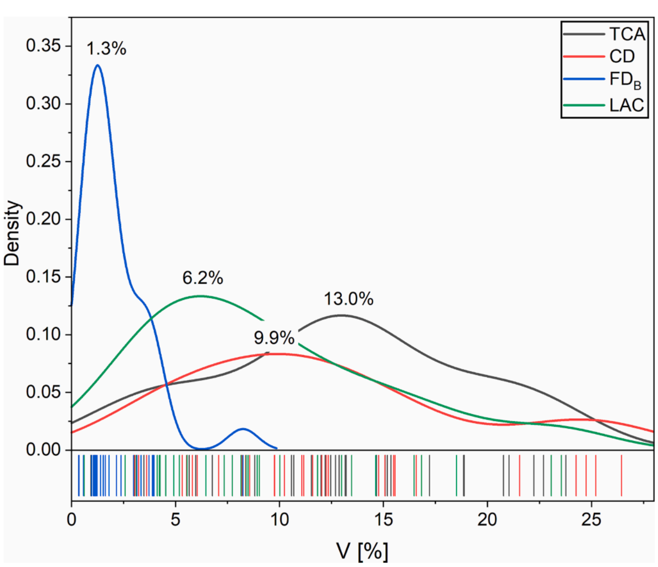


**Fig. 6.** Density distribution of the coefficient of variation (V) for the TCA, CD, $FD_B$, and LAC.

allows to assess the degree of variability of individual parameters within the analyzed series of samples. In this context, the measures of fractal dimension, i.e., $FD_B$ and LAC, were characterized by the least variability. It is worth noting here that studies by other authors [54] indicate that even very small differences in $FD_B$ results are statistically significant. Thus, this is a parameter with which it is possible to detect and determine even very small but significant differences in the degree of CPs development of cement pastes with MWCNTs.

Analyzing the effect of MWCNTs content on the CPs structure, it was found that the effect varied depending on the loading temperature. Tab. 2 shows the relative percentage difference for each series, differing in MWCNTs content, with respect to the reference series (C-0). The changes considered favorable and unfavorable (in green and red, respectively) have been color-coded, i.e., the overall decrease in the number and area occupied by cracks, as well as the decrease in the complexity of the CP structure, were considered favorable. It was found that the higher the content of MWCNTs, the greater the differences in CP structure, with respect to the reference series. Initially, an unfavorable increase in TCA and CD was observed up to 300 °C, ranging from 15.0 to 59.8 % and 5.6–51.2 %, respectively. At 300 °C, the series with the highest amount of MWCNTs, i.e., C-0.2 and C-0.3, were unfavorably characterized by a higher amount and area of cracks on the cement paste surface. In this case, TCA and CD values were obtained higher by 10.3–27.5 %. For formulations with a lower content of MWCNTs, the TCA and CD values oscillated around the values as for the C-0 series (changes in the range of −6.8–10.4 %, respectively). Similar results were obtained for samples loaded at 400 °C, i.e., the differences in TCA and CD values were in the range of −9.5–11.9 % relative to the reference value. On the other hand, at 500 °C and 600 °C, a clearly positive effect of the presence of MWCNTs on the microstructure of the cement matrix was noted, as a decrease in the values of TCA and CD in the best case by as much as 41.5 % relative to the C-0 series was obtained. Such a state of affairs is important in the case of the tightness of the cement matrix since a less cracked cement matrix offers more resistance to the penetration of harmful substances deep into its microstructure. This has the effect of improving the durability of the cement paste at elevated temperatures. Similar results were achieved in study by Lepech and Li [55], who observed an increase in normalized water permeability with an increase in crack opening width. In a study by Sikora et al [56], a decrease in the number of cracks was observed for cement pastes with MWCNTs exposed to elevated temperatures, which is also consistent with the results of the present study.

Analyzing the effect of MWCNTs on the change in the CPs complexity, significant differences were found, relative to the reference series, only at the highest temperature tested, i.e., 600 °C. $FD_B$ values were lower by an average of 2.4–8.4 %, and as in the case of TCA and CD, the greatest differences were obtained for the series with the highest amount of MWCNTs – C-0.3. At the other temperatures, changes in $FD_B$ values were in the range −1.9–5.9 %. In the case of LAC, there was no clear relation with the content of MWCNTs. Differences in LAC values were in a wide range of –22.2–13.4 % relative to the C-0 series, with no clear trend.

### 3.3. Depth of cracks

In order to determine the depth of cracks as a function of temperature, cross-sections of specimens of three series, i.e., C-0, C-0.1 and C-0.3, were analyzed. Fig. 7 shows cross-sections of specimens of the C-0.3 series. Characteristic for all the studied series was the increasing depth of cracks as the thermal load increased, as shown in Fig. 8. Average crack depth (ACD) was measured in the direction perpendicular to the edge of the specimen. It was determined that the largest possible crack depth was 20 mm, which is half of the cross-sectional dimension of the test specimen. The results indicated that in the range from 50 °C to 500 °C there was a relatively uniform increase in ACD from values of 2.2–2.7 mm to 5.0–6.2 mm. On the other hand, after 600 °C, cracks also passed

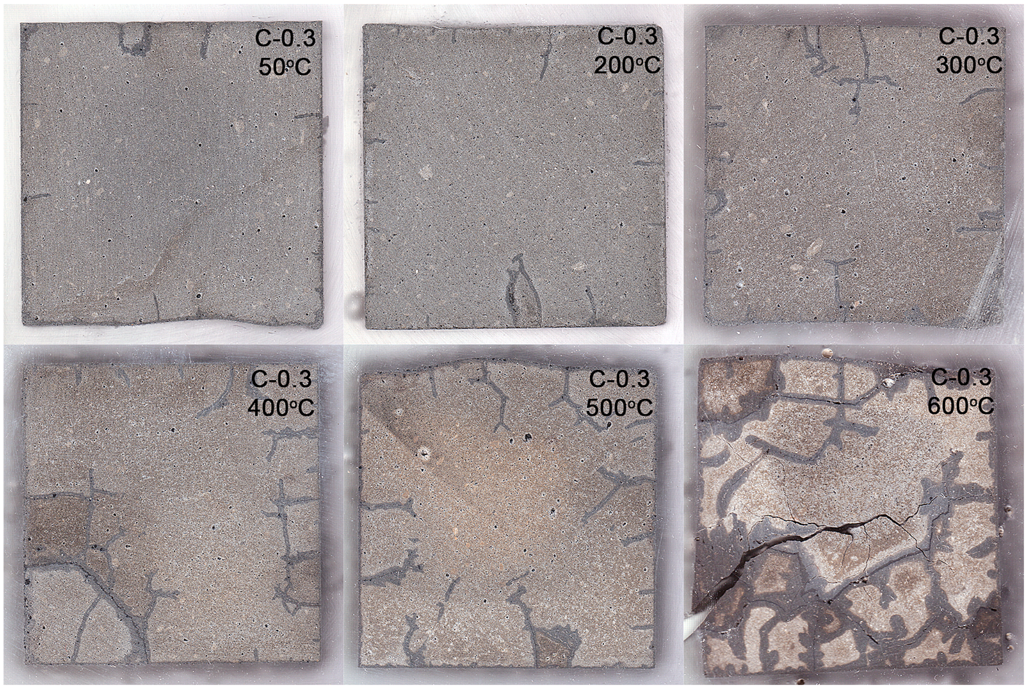


**Fig. 7.** Cross-sections of the sample with the highest MWCNTs content – C-0.3, as a function of the loading temperature.

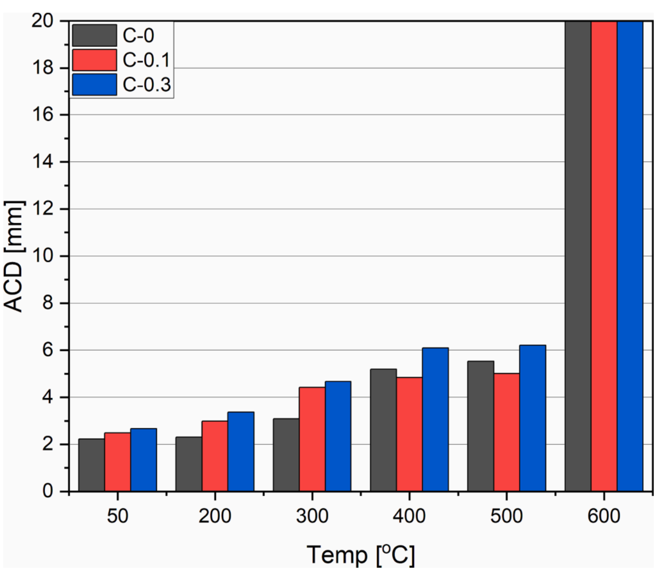


**Fig. 8.** Average crack depth (ACD) depending on the loading temperature.

through the center of the cross-section in all series, so the maximum ACD value was recorded. Modified cement pastes were characterized by residual integrity at this temperature, which strongly negatively affected the mechanical properties. In terms of limiting the depth of cracks, the effect of MWCNTs varied and depended on the loading temperature. Initially after thermal loading, the ACD values of the series with MWCNTs were on the average 15.7 %, 37.4 %, and 47.2 % higher compared to C-0, for 50 °C, 200 °C, and 300 °C, respectively. In contrast, at 400 °C and 500 °C, there was a significant decrease in this difference to 5.2 % (400 °C) and 1.5 % (500 °C). Similar to the results of the CPs analysis, the more favorable effect of using MWCNTs was observed only above 400 °C. The greater depth of cracks in the cement paste with MWCNTs may be due to the fact that there were undispersed clusters of MWCNTs present in the cement matrix, which were weakly bounded to the cement hydration products. These clusters are shown in Fig. 9. The sites of concentration of MWCNTs in this case represented areas of very weak cohesion, through which there was an increased intensity of crack propagation into the material. This effect was greater the higher the concentration of MWCNTs in the volume of the cement matrix – the ACD for C-0.3 was higher than for C-0.1. Studies by other authors [31,56] confirm that only a very good dispersion of MWCNTs in the microstructure of the cement matrix is a guarantee of a significant improvement in its mechanical properties and fracture resistance.

## 4. Conclusions

This article presents the effect of MWCNTs on the basic mechanical properties and CPs structure of cement pastes subjected to elevated temperatures. In the course of the research and analysis carried out, the final conclusions are formulated:

- In terms of mechanical strength, the most favorable results were observed for 0.05 wt% MWCNTs content. The $f_c$ values were on average higher by 7.8 % compared to the reference series (C-0).
- The presence of MWCNTs caused an increase in UPV values in the range of 4.8–7.9 % with respect to C-0. The reason for this is the sealing effect of the cement matrix. The relationships of UPV-$f_c$ and UPV-$f_{cf}$ were characterized by a very high correlation (Pearson's correlation coefficient values of 0.94 and 0.92, respectively).
- In the context of reducing the CPs development of cement paste with MWCNTs, a positive effect was noted only for temperatures of 500 °C and 600 °C. In the best case, a reduction of TCA and CD values by as much as 41 % was obtained.
- According to the available literature data, lacunarity (LAC) was used for the first time as an alternative measure of the fractal dimension to describe the morphology of thermally induced CPs. LAC had the highest correlation (inverse) with the mechanical properties of cement pastes, e.g., the Pearson's correlation coefficient for the LAC-$f_c$ and LAC-UPV relationships was −0.90 and −0.91, respectively.
- The presence of MWCNTs initially caused an increase in ACD values, by as much as 47.2 % at 300 °C. At higher temperatures the ACD values were found to decrease to the level obtained by the reference


**Fig. 9.** Structure of cement matrix in a cross-section: a) C-0; b) C-0.1; c) C-0.3; visible clusters of MWCNTs (in the form of black dots) as their content increases.

series (C-0). It was found that the greater depth of cracks in the cement paste with MWCNTs may be due to the fact that with their increasing content, larger and larger clusters of undispersed MWCNTs were noticed, which were poorly bonded to the hydration products of the cement.

## CRediT authorship contribution statement

**Maciej Szeląg:** Writing – review & editing, Writing – original draft, Visualization, Supervision, Project administration, Methodology, Investigation, Funding acquisition, Conceptualization. **Magdalena Rajczakowska:** Writing – review & editing, Validation, Resources, Methodology, Investigation, Data curation. **Patryk Rumiński:** Writing – original draft, Visualization, Software, Formal analysis, Data curation. **Andrzej Cwirzen:** Writing – review & editing, Validation, Resources, Formal analysis.

## Declaration of Competing Interest

The authors declare that they have no known competing financial interests or personal relationships that could have appeared to influence the work reported in this paper.

## Data availability

Data will be made available on request.

## Acknowledgements

This work was financially supported by the Polish National Agency for Academic Exchange under the Bekker programme, PPN/BEK/2020/1/00014/U/DRAFT/00001.

## References

[1] C.M. Shea, R. Grinde, B. Elmslie, Nanotechnology as general-purpose technology: empirical evidence and implications, Tech. Anal. Strat. Manag. 23 (2) (2011) 175–192.
[2] B. Bhushan, Introduction to nanotechnology, Springer Handbook of Nanotechnology (2017) 1–19.
[3] F. Kreuchauff, N. Teichert, Nanotechnology as general purpose technology, KIT Working Paper Series, Economics (2014).
[4] S.K. Sahoo, The present and future of nanotechnology in human health care, in: J.J. P.S. Parveen (Ed.), Nanomedicine: Nanotechnology, Biology and Medicine, 2007, pp. 20–31.
[5] C.S. Rajan, Nanotechnology in groundwater remediation, International Journal of Environmental Science and Development (2011).
[6] S. Dong, Nickel Plated Carbon Nanotubes Reinforcing Concrete Composites: from Nano/micro Structures to Macro Mechanical Properties, Applied Science and Manufacturing, Composites Part A, 2021.
[7] S.S.-u.-H. Gillani, A. Khitab, S. Ahmad, R.A. Khushnood, G.A. Ferro, S.M.S. Kazmi, L.A. Qureshi, L. Restuccia, Improving the mechanical performance of cement composites by carbon nanotubes addition, Procedia Structural Integrity 3 (2017) 11-17.
[8] T. Manzur, Potential of carbon nanotube reinforced cement composites as concrete repair material, in: M.A.B.E. N. Yazdani (Ed.) Journal of Nanomaterials, 2016, p. 2.
[9] L. Coppola, Electrical Properties of Carbon Nanotubes Cement Composites for Monitoring Stress Conditions in Concrete Structures, in: F.C. A. Buoso (Ed.) Applied Mechanics and Materials, 2011, pp. 118-123.
[10] D. Micheli, Electromagnetic characterization and shielding effectiveness of concrete composite reinforced with carbon nanotubes in the mobile phones frequency band, in: A.V. R. Pastore, R.B. Morles, M. Marchetti, A. Delfini, F. Moglie, V. Mariani Primiani (Ed.) Materials Science and Engineering: B, 2014, pp. 119-129.
[11] P. Zhang, Influence of Carbon Nanotube on Properties of Concrete: A Review, Construction and Building Materials, 2023.
[12] A. Sedaghatdoost, Mechanical properties of Portland cement mortar containing multi-walled carbon nanotubes at elevated temperatures, in: K. Behfarnia (Ed.) Construction and Building Materials, 2018, pp. 482-489.
[13] M.T. Afzal, Influence of Carbon Nano Fibers (CNF) on the Performance of High Strength Concrete Exposed to Elevated Temperatures, Construction and Building Materials, 2021.
[14] J. Foldyna, Dispersion of Carbon Nanotubes for Application in Cement Composites, in: M.Z. V. Foldyna (Ed.) Procedia Engineering, 2016, pp. 94-99.
[15] F.T. Isfahani, Dispersion of multi-walled carbon nanotubes and its effects on the properties of cement composites, in: E.R. W. Li (Ed.) Cement and Concrete Composites 2016, pp. 154-163.
[16] O. Mendoza, Influence of super plasticizer and Ca(OH)2 on the stability of functionalized multi-walled carbon nanotubes dispersions for cement composites applications, in: J.I.T. G. Sierra (Ed.) Construction and Building Materials, 2013, pp. 771-778.
[17] S. Parveen, Microstructure and mechanical properties of carbon nanotube reinforced cementitious composites developed using a novel dispersion technique, in: R.F. S. Rana, M. C. Paiva (Ed.) Cement and Concrete Research, 2015, pp. 215-227.
[18] W.L. Baloch, R.A. Khushnood, W. Khaliq, Influence of multi-walled carbon nanotubes on the residual performance of concrete exposed to high temperatures, Constr. Build. Mater. 185 (2018) 44–56.
[19] A. Karaipekli, Thermal characteristics of expanded perlite/paraffin composite phase change material with enhanced thermal conductivity using carbon nanotubes, in: A.S. A. Biçer, V. V. Tyagi (Ed.) Energy Conversion and Management, 2017, pp. 373-381.
[20] M.K. Hassanzadeh-Aghdam, Effect of adding carbon nanotubes on the thermal conductivity of steel fiber-reinforced concrete, in: M.S. M. J. Mahmoodi (Ed.) Composites Part B: Engineering, 2019.
[21] Y. Yao, Mechanical Properties and Failure Mechanism of Carbon Nanotube Concrete at High Temperatures, Construction and Building Materials, 2021.
[22] K. Sakr, Effect of high temperature or fire on heavy weight concrete properties, in: E. El-Hakim (Ed.) Cement and Concrete Research, 2005, pp. 590-596.
[23] I. Khan, Prediction of reinforcement corrosion using corrosion induced cracks width in corroded reinforced concrete beams, in: A.C. R. Francois (Ed.) Cement and Concrete Research, 2014, pp. 84-96.
[24] K. Tosun-Felekoglu, Effects of fibre hybridization on multiple cracking potential of cement-based composites under flexural loading, in: B. Felekoglu (Ed.) Construction and Building Materials, 2013, pp. 15-20.
[25] N. Zhuang, Cracking behavior of reinforced concrete piles externally bonded with carbon fiber reinforced polymer in a marine environment, in: Y.Z. H. Dong, D. Chen (Ed.) Construction and Building Materials, 2018, pp. 1154-1162.
[26] C. Wagner, Water permeability of cracked strain-hardening cement-based composites, in: V.S. B. Villmann, V. Mechtcherine (Ed.) Cement & Concrete Composites, 2017, pp. 234-241.
[27] M. Szelag, Properties of cracking patterns of multi-walled carbon nanotube-reinforced cement matrix, Materials (2019).
[28] K. Kim, Evaluation of pore structures and cracking in cement paste exposed to elevated temperatures by X-ray computed tomography, in: K.P. T. Yun (Ed.) Cement and Concrete Research, 2013, pp. 34-40.
[29] M. Rajczakowska, M. Szeląg, K. Habermehl-Cwirzen, H. Hedlund, A. Cwirzen, Autogenous self-healing of thermally damaged cement paste with carbon nanomaterials subjected to different environmental stimulators, Journal of Building Engineering 72 (2023), 106619.
[30] S. Xu, Mechanical properties and microstructure of multi-walled carbon nanotube-reinforced cement paste, in: Q.L. J. Liu (Ed.) Construction and Building Materials, 2015, pp. 16-23.

[31] J. Zhang, Cement paste with well-dispersed multi-walled carbon nanotubes: Mechanism and performance, in: J.Z. Y. Ke, Q. Han, B. Dong (Ed.) Construction and Building Materials, 2020.
[32] S. Arrechea, E.M. Guerrero-Gutiérrez, L. Velásquez, J. Cardona, R. Posadas, K. Callejas, S. Torres, R. Díaz, C. Barrientos, E. García, Effect of additions of multiwall carbon nanotubes (MWCNT, MWCNT-COOH and MWCNT-Thiazol) in mechanical compression properties of a cement-based material, Materialia 11 (2020), 100739.
[33] M. Szeląg, The application of NDT techniques to examination of thermally-induced cracking patterns of brick powder-Portland cement matrix, Developments in the Built Environ. (2022).
[34] M. Szeląg, Intelligent prediction modeling of the post-heating mechanical performance of the brick powder modified cement paste based on the cracking patterns properties, Case Studies Constr. Mater. (2021).
[35] EN 12390-5. Testing Hardened Concrete - Part 5: Flexural Strength of Test Specimens, London, UK, 2009.
[36] EN 12390-3. Testing Hardened Concrete - Part 3: Compressive Strength of Test Specimens, London, UK, 2002.
[37] I. Arganda-Carreras, Trainable Weka Segmentation: a machine learning tool for microscopy pixel classification, in: C.R. V. Kaynig, K. Eliceiri, J. Schindelin, A. Cardona, H. Seung (Ed.) Bioinformatics, 2017, pp. 2424-2426.
[38] M. Szeląg, Application of an Automated Digital Image-Processing Method for Quantitative Assessment of Cracking Patterns in a Lime Cement Matrix, Sensors, 2020.
[39] M. Szeląg, Fractal characterization of thermal cracking patterns and fracture zone in low-alkali cement matrix modified with microsilica, Cem. Concr. Compos. (2020).
[40] A. Karperien, FracLac for ImageJ, http://rsb.info.nih.gov/ij/plugins/fraclac/FLHelp/Introduction.htm, pp. 1999-2013.
[41] A. Chaipanich, Compressive strength and microstructure of carbon nanotubes–fly ash cement composites, in: W.W. T. Nochaiya, P. Torkittikul (Ed.) 2010, pp. 1063-1067.
[42] S. Lim, P. Mondal, Effects of nanosilica addition on increased thermal stability of cement-based composite, ACI Mater. J. 112 (2) (2015) 305–315.
[43] M.R. Irshidat, Hybrid effect of carbon nanotubes and polypropylene microfibers on fire resistance, thermal characteristics and microstructure of cementitious composites, in: M.R. N. Al-Nuaimi (Ed.) Construction and Building Materials, 2021.
[44] X. Cui, Mechanical properties and reinforcing mechanisms of cementitious composites with different types of multiwalled carbon nanotubes, in: Q.Z. B. Han, X. Yu, S. Dong, L. Zhang, J. Ou (Ed.) Composites Part A: Applied Science and Manufacturing, 2017, pp. 131-147.
[45] D. Leonavičius, The effect of multi-walled carbon nanotubes on the rheological properties and hydration process of cement pastes, in: G.G. I. Pundienė, J. Pranckevičienė, M. Kligys, A. Kairytė (Ed.) Construction and Building Materials, 2018, pp. 947-954.
[46] M. Szeląg, The application of NDT techniques to examination of thermally-induced cracking patterns of brick powder-Portland cement matrix, Developments in the Built Environment 12 (2022), 100104.
[47] B. Demirel, O. Kelestemur, Effect of elevated temperature on the mechanical properties of concrete produced with finely ground pumice and silica fume, Fire Saf. J. 45 (6–8) (2010) 385–391.
[48] P. Prochoń, Bound water content measurement in cement pastes by stoichiometric and gravimetric analyses, in: T. Piotrowski (Ed.) Journal of Building Chemistry, 2016, pp. 18-25.
[49] N. Recho, Fracture Mechanics and crack growth, John Wiley & Sons, 2012.
[50] D.J. Naus, The effect of elevated temperature on concrete materials and structures - a literature review (No. ORNL/TM-2005/533), Oak Ridge, Oak Ridge National Laboratory, 2006.
[51] A. Farhidzadeh, Damage Assessment of Reinforced Concrete Structures Using Fractal Analysis of Residual Crack Patterns, in: A.M. E. Dehghan-Niri, S. Salamone, A. Whittaker (Ed.) Experimental Mechanics, 2013, pp. 1607-1619.
[52] K. Yu, Determination of the softening curve and fracture toughness of high-strength concrete exposed to high temperature, in: Z.L. J. Yu, Q. Chen (Ed.) Engineering Fracture Mechanics, 2015, pp. 156-169.
[53] D. Sebok, Fast and accurate lacunarity calculation for large 3D micro-CT datasets, in: I.S. L. Vasarhelyi, R. Vajtai, Z. Konya, A. Kukovecz (Ed.) Acta Materialia, 2021.
[54] A. Rezaie, Sensitivity analysis of fractal dimensions of crack maps on concrete and masonry walls, in: K.B. A. Mauron (Ed.) Automation in Construction, 2020.
[55] M. Lepech, Water permeability of engineered cementitious composites, in: V. Li (Ed.) Cement & Concrete Composites, 2009, pp. 744-753.
[56] P. Sikora, Mechanical and microstructural properties of cement pastes containing carbon nanotubes and carbon nanotube-silica core-shell structures, exposed to elevated temperature, in: S.C. M. Abd Elrahman, K. Cendrowski, E. Mijowska, D. Stephan (Ed.) Cement & Concrete Composites, 2019, pp. 193-204.